Simulation of Raman Amplification*

Roland W. Freund
Bell Laboratories
Lucent Technologies
Room 2C–525
700 Mountain Avenue
Murray Hill, NJ 07974–0636
e-mail: freund@research.bell-labs.com

Abstract

We present a general formulation of the system of differential equations that describe the power evolution in Raman fiber amplifiers. The solutions of these equations model the forward and backward power spectral densities of Raman amplifiers as functions of position along the fiber, time, and frequency. The time dependence of these equations allows the use of them for simulation of transient effects. The frequency dependence allows the use of these equations for a fully-coupled signal and noise analysis, both in the steady-state and the time-dependent case. The equations include terms that model stimulated Raman scattering, spontaneous Raman scattering due to both Stokes and anti-Stokes emission and absorption, and Rayleigh scattering. We also outline a Galerkin approach for the frequency discretization of the equations.

1 Introduction

It has long been known that stimulated Raman scattering can be employed to build amplifiers for compensating fiber loss in optical transmission systems. We refer the reader to [8, 20, 21, 22], [1, Chapter 8], [27, Chapter 3], and the references given there. Raman amplifiers use the fiber itself as the amplification medium. Raman pump power is launched into the fiber and then transferred to the signals via Raman scattering.

In recent years, there has been a lot of interest in Raman amplification; see, e.g., [5, 24, 25, 37, 38], the survey papers [4, 22, 28], and the references given there.

There are two main reasons for this renewed interest in Raman amplification. First, the Raman effect has a broad gain curve, which makes it very attractive for today's broadband DWDM (dense wavelength-division multiplexing) systems [12]. By employing a small number of Raman pumps, operating at different frequencies, it is possible to provide sufficient gain throughout the whole signal band. In Figure 1 we display the typical Raman gain curves for a state-of-the-art DWDM system with six Raman pumps. Note that the gain curves are normalized so that the maximal gain for each curve is one. Also shown in Figure 1 is a typical set of channel frequencies in such a DWDM system. There are 128 channels from 186.50 THz to 192.85 THz, with 50 GHz spacing.

*Numerical Analysis Manuscript No. 02–4–37, Bell Laboratories, Murray Hill, New Jersey, November 2002. Available on WWW at `http://cm.bell-labs.com/cs/doc/02`.

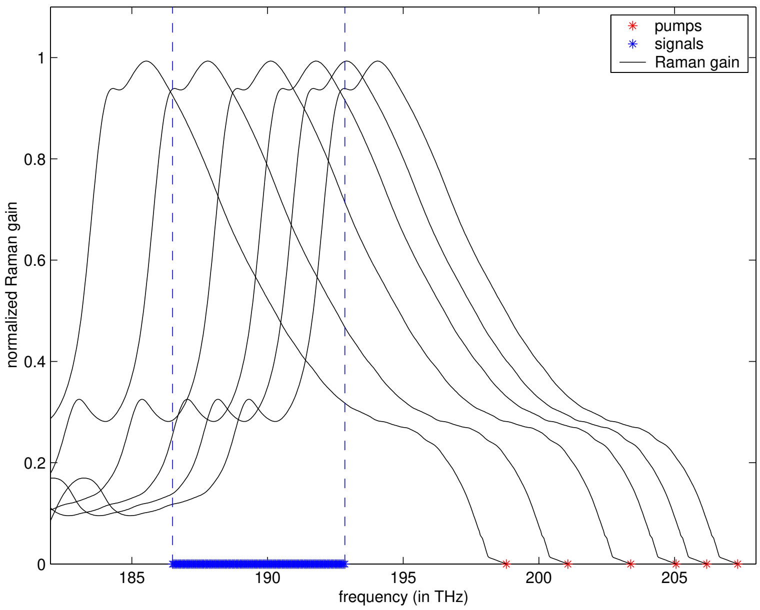

Figure 1: Raman gain of six pumps operating at different frequencies

Second, Raman amplifiers require pumps with output of several hundreds of milliwatts. Semiconductor pump lasers with such power outputs have now become commercially available at an appropriate cost, and thus Raman amplification has become feasible.

As indicated above, Raman amplifiers for broadband systems employ multiple pumps. An important problem in the design of Raman amplifiers is the choice of the frequencies and the power ranges of these multiple pumps. These design parameters need to be chosen such that the pumps provide enough gain for all possible channel configurations, while at the same time the noise floor is kept low. The complexity of this design problem is such that the use of numerical simulation has become an absolute necessity. For a more general overview of photonic simulation tools, we refer the reader to [16].

The need for numerical simulation also arises in the development and testing of control algorithms for Raman amplifiers. For example, the powers of the Raman pumps need to be adjusted dynamically, so that signal powers are as flat as possible, relative to some given power target. A simulation platform, such as the one described in [9], can be used to develop and test algorithms for Raman control.

Another important control problem for Raman amplifiers is the suppression of power transients due to catastrophic events such as fiber cuts or component failures; see, e.g., [2, 3, 6, 11, 34].

The above design and control problems require the simulation of the power evolution of forward and backward propagating waves along the fiber. The equations describing this power evolution are in principle well known, but, surprisingly, most publications seem to contain incomplete or even faulty statements of these equations; see, e.g., [11, 14, 17, 19, 24, 38]. For example, the widely-referenced equations in [14] only account for spontaneous Stokes, but not anti-Stokes, scattering, even though, as pointed out in [24], the effects of Stokes and anti-Stokes scattering are of comparable size for the closely-spaced channels of today's DWDM systems. Many papers consider only the steady-state case, or simplified versions of the equations for the

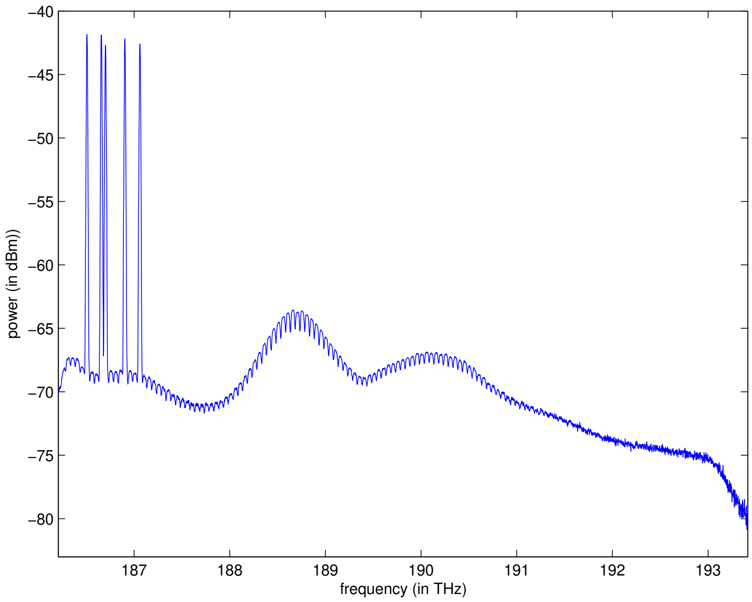

Figure 2: Power spectrum for a case of five signal channels

noise-less case.

The purpose of this paper is to present the most general formulation of the system of differential equations that describe the power evolution in Raman fiber amplifiers. The solutions of these equations model the forward and backward power spectral densities of Raman amplifiers as functions of position along the fiber, time, and frequency. The equations include terms that model stimulated Raman scattering, spontaneous Raman scattering due to both Stokes and anti-Stokes emission and absorption, and Rayleigh scattering. No distinction is made between signal or pump power and noise, and the equations are formulated for total power (signal, pump, and noise) spectral densities. This approach allows to directly simulate the power spectra, such as the one in Figure 2, that are measured by optical monitoring devices in actual DWDM systems. Figure 2 shows the power spectrum measured at the end of an outside-plant fiber span of a DWDM system with a signal band from 186.50 THz to 192.85 THz. In the case displayed in Figure 2 only five signal channels (at 186.50, 186.65, 186.70, 186.90, and 187.05 THz) are present.

The remainder of this paper is organized as follows. In Section 2 we introduce some notation and briefly describe the gain terms for simulated and spontaneous Raman scattering. In Section 3 we state the system of differential equations that describe the power evolution in Raman fiber amplifiers. In Section 4 we sketch a Galerkin approach for the frequency discretization of these equations. Finally, we make some concluding remarks in Section 5.

2 Preliminaries

In this section we introduce the notation that is used in our formulation of the equations for power evolution of Raman amplifiers. We also describe the gain terms for the various flavors of Raman scattering.

2.1 Raman gain

We denote by

$$g_{\mathrm{R}}(\Delta\zeta;\zeta), \quad \Delta\zeta \geq 0, \tag{1}$$

the Raman gain spectrum for a pump at frequency ζ. Here we assume that the pump is depolarized; the case of polarized pumps is discussed briefly in Section 2.4 below. The function $g_{\mathrm{R}}(\Delta\zeta;\zeta)$ is known to depend linearly on the pump frequency:

$$g_{\mathrm{R}}(\Delta\zeta;\zeta) = \frac{\zeta}{\zeta_{\mathrm{ref}}}\, g_{\mathrm{R}}(\Delta\zeta;\zeta_{\mathrm{ref}}) \quad \text{for all} \quad \Delta\zeta \geq 0; \tag{2}$$

see, e.g., [32, 33]. In practice, the Raman gain spectrum is measured for a reference pump frequency, ζ_{ref}. The relation (2) is then used to obtain the Raman gain spectrum for any pump frequency ζ.

We denote by $A_{\mathrm{R}}(\nu,\zeta)$ the Raman effective area; see, e.g., [35, 36]. The actual "gain" function that is used for our formulation of the power-evolution equations is given by

$$g(\nu,\zeta) := \frac{g_{\mathrm{R}}\left(|\zeta-\nu|;\zeta\right)}{A_{\mathrm{R}}(\nu,\zeta)}. \tag{3}$$

We remark that the second argument of the function $g(\cdot,\cdot)$ is the frequency of the wave acting as the pump in Raman scattering.

The values of the function (3) are usually given only for a fixed pump frequency, say ζ_{ref}. The values of $g(\nu,\zeta)$ for any pair of frequencies ζ, ν with

$$|\zeta-\nu| \leq \zeta_{\mathrm{ref}} \tag{4}$$

can then be obtained via the relation

$$g(\nu,\zeta) = g\left(\zeta_{\mathrm{ref}} - |\zeta-\nu|, \zeta_{\mathrm{ref}}\right) \frac{\zeta}{\zeta_{\mathrm{ref}}} \frac{A_{\mathrm{R}}\left(\zeta_{\mathrm{ref}} - |\zeta-\nu|, \zeta_{\mathrm{ref}}\right)}{A_{\mathrm{R}}(\nu,\zeta)}, \tag{5}$$

which readily follows from (3) and (2). Note that for practical systems, $|\zeta-\nu| < 40$ THz and $\zeta_{\mathrm{ref}} > 190$ THz, and thus condition (4) is always satisfied. The Raman effective area $A_{\mathrm{R}}(\nu,\zeta)$ is usually approximated by

$$A_{\mathrm{R}}(\nu,\zeta) \approx \frac{1}{2}\big(A_{\mathrm{eff}}(\nu) + A_{\mathrm{eff}}(\zeta)\big), \tag{6}$$

where $A_{\mathrm{eff}}(\nu)$ denotes the fiber's effective core area. Using (6), we obtain the approximation

$$g(\nu,\zeta) \approx g\left(\zeta_{\mathrm{ref}} - |\zeta-\nu|, \zeta_{\mathrm{ref}}\right) \frac{\zeta}{\zeta_{\mathrm{ref}}} \frac{A_{\mathrm{eff}}\left(\zeta_{\mathrm{ref}} - |\zeta-\nu|\right) + A_{\mathrm{eff}}\left(\zeta_{\mathrm{ref}}\right)}{A_{\mathrm{eff}}(\nu) + A_{\mathrm{eff}}(\zeta)}. \tag{7}$$

In practice, one provides values for the function

$$g\left(\Delta\nu, \zeta_{\mathrm{ref}}\right), \quad 0 \leq \Delta\nu \leq 40\mathrm{THz}, \tag{8}$$

along with the reference frequency ζ_{ref}, and values for the function

$$A_{\mathrm{eff}}(\nu), \quad \nu \geq 0. \tag{9}$$

The approximation (7) is then employed to obtain values of $g(\nu,\zeta)$ for any ν and ζ.

2.2 Power spectral density

We formulate the equation for Raman amplification in terms of power spectral densities with respect to frequency. More precisely,

$$\rho(z, t, \nu), \quad \nu \geq 0, \tag{10}$$

denotes the power spectral density at position z along the fiber and time t. The actual power in a frequency interval $[\nu_1, \nu_2]$ is then given by

$$P(z, t; \nu_1, \nu_2) = \int_{\nu_1}^{\nu_2} \rho(z, t, \nu)\, d\nu. \tag{11}$$

We use superscripts "+" and "−" to distinguish forward and backward propagating waves. Thus, $\rho^+(z, t, \nu)$ and $\rho^-(z, t, \nu)$ denote the forward and backward power spectral densities, respectively.

2.3 Gain terms for Raman scattering

Next, we briefly review the gain terms for the various flavors of Raman scattering. For derivations and more detailed descriptions of these terms, we refer the reader to [18, Chapter 5], [23], [29, Chapter 10].

For the remainder of this subsection, we consider two waves at frequencies ν and ζ with (forward or backward) power spectral densities $\rho(z, t, \nu)$ and $\rho(z, t, \zeta)$, respectively. Moreover, we assume that $\zeta > \nu$.

For stimulated Raman scattering, the wave at the higher frequency ζ acts as a pump for the wave at lower frequency ν. The gain for the wave at ν is proportional to

$$g(\nu, \zeta)\, \rho(z, t, \nu)\, \rho(z, t, \zeta). \tag{12}$$

The corresponding loss for the pump at ζ is proportional to

$$-\frac{\zeta}{\nu}\, g(\nu, \zeta)\, \rho(z, t, \nu)\, \rho(z, t, \zeta). \tag{13}$$

The difference $\zeta/\nu - 1$ between the factors in (13) and (12) accounts for pump energy that is absorbed by the fiber in the form of molecular vibrations. Note that the gain terms for stimulated Raman scattering are independent of temperature.

Next, we discuss spontaneous Raman scattering. For Stokes scattering, an incident pump photon scatters off from a molecule creating a photon with lower frequency. The difference in energy of the pump photon and the scattered photon leaves the molecule in an excited vibrational state. For anti-Stokes scattering, an incident pump photon scatters off from a molecule in an excited vibrational state, thus de-exciting the molecule and emitting a photon with higher frequency. Both Stokes and anti-Stokes scattering are temperature-dependent. More precisely, the absolute temperature T enters via the quantity

$$n_T(\nu, \zeta) := \frac{1}{\exp\left(h\,|\nu - \zeta|\,/(k_{\mathrm{B}}T)\right) - 1}, \tag{14}$$

where h is Planck's and k_{B} is Boltzmann's constant.

For spontaneous Stokes scattering, the wave at frequency ζ creates scattered photons at lower frequency ν. The associated gain for the wave at ν is proportional to

$$h\nu\, g(\nu,\zeta)\, \rho(z,t,\zeta)\, (1+n_T(\nu,\zeta))\,. \tag{15}$$

The corresponding loss for the wave at ζ is proportional to

$$-h\nu\, \frac{\zeta}{\nu}\, g(\nu,\zeta)\, \rho(z,t,\zeta)\, (1+n_T(\nu,\zeta)) = -h\zeta\, g(\nu,\zeta)\, \rho(z,t,\zeta)\, (1+n_T(\nu,\zeta))\,. \tag{16}$$

For spontaneous anti-Stokes scattering, the wave at frequency ν creates scattered photons at higher frequency ζ. The associated gain for the wave at ζ is proportional to

$$h\zeta\, g(\nu,\zeta)\, \rho(z,t,\nu)\, n_T(\nu,\zeta). \tag{17}$$

The corresponding loss for the wave at ν is proportional to

$$-h\zeta\, \frac{\nu}{\zeta}\, g(\nu,\zeta)\, \rho(z,t,\nu)\, n_T(\nu,\zeta) = -h\nu\, g(\nu,\zeta)\, \rho(z,t,\nu)\, n_T(\nu,\zeta). \tag{18}$$

Note that the gain for spontaneous Stokes and anti-Stokes scattering is proportional to

$$1+n_T(\nu,\zeta) \quad \text{and} \quad n_T(\nu,\zeta), \tag{19}$$

respectively. Therefore, gain due to spontaneous Stokes scattering is always higher than gain due to spontaneous anti-Stokes scattering. However, for waves with close frequencies ν and ζ, $n_T(\nu,\zeta) \gg 1$ and hence the two factors (19) are close. For example, for $T = 300$ K and $|\nu - \zeta| = 100$ GHz, we have

$$1+n_T(\nu,\zeta) = 63.025894... \quad \text{and} \quad n_T(\nu,\zeta) = 62.025894... \,.$$

2.4 Polarization

Recall that the Raman gain (1) assumes a depolarized pump. For stimulated Raman scattering, if the pump and the wave on which it acts are polarized, then the stimulated Raman gain terms (12) and (13) in Section 2.3 need to be multiplied by a factor that depends on the relative polarization between pump and the wave on which it acts; see, e.g., [31]. For example, if both these waves have parallel linear polarizations, then maximum Raman gain occurs and the gain terms (12) and (13) need to be multiplied by a factor of 2. For spontaneous Raman scattering, the generated photon has the same polarization as the incident pump photon; see, e.g., [23]. Thus, each of the spontaneous Raman gain terms (15)–(18) in Section 2.3 need to be multiplied by a factor of 2.

To properly formulate the power-evolution equations for Raman amplifiers in the general case, we need some notation for the Raman gain modification due to relative polarization between waves. We use $K(\nu,\zeta)$ to denote the inverse of the multiplicative factor for Raman gain terms for two waves at frequencies ν and ζ. For example, if both waves are randomly polarized relative to each other, then $K(\nu,\zeta) = 1$, and if both waves have parallel linear polarizations, then $K(\nu,\zeta) = 1/2$.

Furthermore, since we distinguish between forward and backward propagating waves, which in general can have different polarizations, we use the following functions

$$K^{++}(\nu,\zeta), \quad K^{+-}(\nu,\zeta), \quad K^{-+}(\nu,\zeta), \quad K^{--}(\nu,\zeta). \tag{20}$$

Here, the first superscript "+" or "−" means that the wave with frequency ν propagates forward or backward, respectively, along the fiber. Similarly, the second superscript "+" or "−" indicates the direction of the wave with frequency ζ. We remark that, in principle, the polarization terms (20) could also be functions of the position along the fiber, z, and of time t. However, in our notation, we suppress this potential dependence on z and t.

Note that the Raman systems in which we are mainly interested employ depolarized Raman pumps. Moreover, even though signals are linearly polarized, the relative polarization between them becomes random as they propagate along the fiber; see [31]. Hence, for such systems, we have

$$K^{++}(\nu,\zeta) = K^{+-}(\nu,\zeta) = K^{-+}(\nu,\zeta) = K^{--}(\nu,\zeta) = 1 \quad \text{for all} \quad \nu,\ \zeta. \tag{21}$$

3 The general equations

After these preliminaries, we are now in a position to formulate the general equations for power evolution in Raman fiber amplifiers.

The equations are partial differential equations (in z and t) for the forward and backward power spectral densities

$$\rho^{+}(z,t,\nu) \quad \text{and} \quad \rho^{-}(z,t,\nu). \tag{22}$$

Here,

$$0 \le z \le L \tag{23}$$

is the position along the fiber, L is the length of the fiber,

$$t \ge 0 \tag{24}$$

is time, and

$$\nu_{\min} \le \nu \le \nu_{\max} \tag{25}$$

is frequency in some frequency window $[\nu_{\min}, \nu_{\max}]$ that should be chosen large enough so that the signal band and the frequency ranges of all Raman pumps are part of this window.

The differential equations for the functions (22) are then as follows:

$$\frac{\partial\rho^+(z,t,\nu)}{\partial z}+\frac{1}{v_{\mathrm{g}}(\nu)}\frac{\partial\rho^+(z,t,\nu)}{\partial t}=-\alpha(\nu)\rho^+(z,t,\nu)+\gamma(\nu)\rho^-(z,t,\nu) \tag{26}$$

$$+\rho^+(z,t,\nu)\int_{\zeta>\nu}g(\nu,\zeta)\left(\frac{\rho^+(z,t,\zeta)}{K^{++}(\nu,\zeta)}+\frac{\rho^-(z,t,\zeta)}{K^{+-}(\nu,\zeta)}\right)d\zeta \tag{27}$$

$$-\rho^+(z,t,\nu)\int_{\zeta<\nu}\frac{\nu}{\zeta}\,g(\zeta,\nu)\left(\frac{\rho^+(z,t,\zeta)}{K^{++}(\nu,\zeta)}+\frac{\rho^-(z,t,\zeta)}{K^{+-}(\nu,\zeta)}\right)d\zeta \tag{28}$$

$$+2h\nu\int_{\zeta>\nu}(1+n_T(\nu,\zeta))\,g(\nu,\zeta)\big(\rho^+(z,t,\zeta)+\rho^-(z,t,\zeta)\big)\,d\zeta \tag{29}$$

$$-4h\nu\,\rho^+(z,t,\nu)\int_{\zeta<\nu}(1+n_T(\nu,\zeta))\,g(\zeta,\nu)\,d\zeta \tag{30}$$

$$+2h\nu\int_{\zeta<\nu}n_T(\nu,\zeta)\,g(\zeta,\nu)\big(\rho^+(z,t,\zeta)+\rho^-(z,t,\zeta)\big)\,d\zeta \tag{31}$$

$$-4h\nu\,\rho^+(z,t,\nu)\int_{\zeta>\nu}n_T(\nu,\zeta)\,g(\nu,\zeta)\,d\zeta, \tag{32}$$

$$\frac{\partial\rho^-(z,t,\nu)}{\partial z}-\frac{1}{v_{\mathrm{g}}(\nu)}\frac{\partial\rho^-(z,t,\nu)}{\partial t}=\alpha(\nu)\rho^-(z,t,\nu)-\gamma(\nu)\rho^+(z,t,\nu) \tag{33}$$

$$-\rho^-(z,t,\nu)\int_{\zeta>\nu}g(\nu,\zeta)\left(\frac{\rho^+(z,t,\zeta)}{K^{-+}(\nu,\zeta)}+\frac{\rho^-(z,t,\zeta)}{K^{--}(\nu,\zeta)}\right)d\zeta \tag{34}$$

$$+\rho^-(z,t,\nu)\int_{\zeta<\nu}\frac{\nu}{\zeta}\,g(\zeta,\nu)\left(\frac{\rho^+(z,t,\zeta)}{K^{-+}(\nu,\zeta)}+\frac{\rho^-(z,t,\zeta)}{K^{--}(\nu,\zeta)}\right)d\zeta \tag{35}$$

$$-2h\nu\int_{\zeta>\nu}(1+n_T(\nu,\zeta))\,g(\nu,\zeta)\big(\rho^+(z,t,\zeta)+\rho^-(z,t,\zeta)\big)\,d\zeta \tag{36}$$

$$+4h\nu\,\rho^-(z,t,\nu)\int_{\zeta<\nu}(1+n_T(\nu,\zeta))\,g(\zeta,\nu)\,d\zeta \tag{37}$$

$$-2h\nu\int_{\zeta<\nu}n_T(\nu,\zeta)\,g(\zeta,\nu)\big(\rho^+(z,t,\zeta)+\rho^-(z,t,\zeta)\big)\,d\zeta \tag{38}$$

$$+4h\nu\,\rho^-(z,t,\nu)\int_{\zeta>\nu}n_T(\nu,\zeta)\,g(\nu,\zeta)\,d\zeta. \tag{39}$$

Note that (26)–(39) is a coupled system of partial differential equations for the unknown functions (22). The system (26)–(39) is completed by initial conditions for ρ^+ at the beginning of the fiber,

$$\rho^+(0,t,\nu)=r_0(t,\nu)\quad\text{for all}\quad t\geq 0\quad\text{and}\quad \nu_{\min}\leq\nu\leq\nu_{\max}, \tag{40}$$

and by initial conditions for ρ^- at the end of the fiber,

$$\rho^-(L,t,\nu) = r_1(t,\nu) \quad \text{for all} \quad t \geq 0 \quad \text{and} \quad \nu_{\min} \leq \nu \leq \nu_{\max}. \tag{41}$$

Here, $r_0(t,\nu)$ and $r_1(t,\nu)$ are given functions.

Note that the terms on the right-hand sides of (26) and (33) represent fiber loss and Rayleigh scattering. The terms (27) and (34) account for gain from higher-frequency waves due to stimulated Raman scattering. The terms (28) and (35) represent loss to lower-frequency waves due to stimulated Raman scattering. The terms (29) and (36) account for gain from higher-frequency waves due to spontaneous Stokes scattering. The terms (30) and (37) represent loss to lower-frequency waves due to spontaneous Stokes scattering. The terms (31) and (38) account for gain from lower-frequency waves due to spontaneous anti-Stokes scattering. The terms (32) and (39) represent loss to higher-frequency waves due to spontaneous anti-Stokes scattering.

Next, we summarize the meaning of the various quantities in the system (26)–(39).

z	position along the fiber
t	time
ν	frequency
$\rho^+(z,t,\nu)$	forward power spectral density
$\rho^-(z,t,\nu)$	backward power spectral density
$v_{\mathrm{g}}(\nu)$	group velocity
$\alpha(\nu)$	attenuation
$\gamma(\nu)$	Rayleigh scattering coefficient
$g(\nu,\zeta)$	Raman gain for pump at frequency ζ as defined in (3), or as approximated by (7)
$K^{\pm\pm}(\nu,\zeta)$	polarization factors (20)
h	Planck's constant
$n_T(\nu,\zeta)$	factor defined in (14)
T	absolute temperature

4 A Galerkin approach for frequency discretization

In this section we describe a Galerkin approach for the frequency discretization of the partial differential equations (26)–(41). In this section we restrict ourselves to the case (21), which is always satisfied for the Raman systems in which we are interested.

4.1 A more compact formulation of the equations

As a first step, we rewrite the partial differential equations equations (26)–(39) (with polarization functions (21)) in a more compact form, which is better suited for the numerical solution of these equations.

To this end, we introduce the following functions:

$$a(\nu,\zeta) := \begin{cases} g(\nu,\zeta) & \text{if } \zeta \geq \nu, \\ -\dfrac{\nu}{\zeta}\, g(\zeta,\nu) & \text{if } \zeta < \nu, \end{cases} \tag{42}$$

$$b_T(\nu,\zeta) := \begin{cases} (1+n_T(\nu,\zeta))\, g(\nu,\zeta) & \text{if } \zeta \geq \nu, \\ n_T(\nu,\zeta)\, g(\zeta,\nu) & \text{if } \zeta < \nu, \end{cases} \tag{43}$$

$$\delta_T(\nu) := \alpha(\nu) + 4h\nu \int_\zeta b_T(\zeta,\nu)\, d\zeta. \tag{44}$$

We remark that

$$a(\nu,\zeta) = 0 \quad \text{and} \quad b_T(\nu,\zeta) = 0 \quad \text{for all} \quad \nu = \zeta,$$

and thus the functions (42) and (43) are continuous for all ν and ζ.

Using (42)–(44), the equations (26)–(39) can be restated as follows:

$$\frac{\partial \rho^+(z,t,\nu)}{\partial z} + \frac{1}{v_{\mathrm{g}}(\nu)} \frac{\partial \rho^+(z,t,\nu)}{\partial t} = -\delta_T(\nu)\, \rho^+(z,t,\nu) + \gamma(\nu)\, \rho^-(z,t,\nu) \tag{45}$$

$$+ \rho^+(z,t,\nu) \int_\zeta a(\nu,\zeta) \left(\rho^+(z,t,\zeta) + \rho^-(z,t,\zeta)\right) d\zeta \tag{46}$$

$$+ 2h\nu \int_\zeta b_T(\nu,\zeta) \left(\rho^+(z,t,\zeta) + \rho^-(z,t,\zeta)\right) d\zeta, \tag{47}$$

$$\frac{\partial \rho^-(z,t,\nu)}{\partial z} - \frac{1}{v_{\mathrm{g}}(\nu)} \frac{\partial \rho^-(z,t,\nu)}{\partial t} = \delta_T(\nu)\, \rho^-(z,t,\nu) - \gamma(\nu)\, \rho^+(z,t,\nu) \tag{48}$$

$$- \rho^-(z,t,\nu) \int_\zeta a(\nu,\zeta) \left(\rho^+(z,t,\zeta) + \rho^-(z,t,\zeta)\right) d\zeta \tag{49}$$

$$- 2h\nu \int_\zeta b_T(\nu,\zeta) \left(\rho^+(z,t,\zeta) + \rho^-(z,t,\zeta)\right) d\zeta. \tag{50}$$

4.2 The general ansatz and the resulting equations

Next, we describe a Galerkin approach for the frequency discretization of the partial differential equations (45)–(50) and the associated initial conditions (40) and (41).

To discretize the equations (45)–(50) in frequency space, one first chooses two sets of basis functions

$$f_0^+(\nu), f_1^+(\nu), \ldots, f_{l^+}^+(\nu) \quad \text{and} \quad f_0^-(\nu), f_1^-(\nu), \ldots, f_{l^-}^-(\nu) \tag{51}$$

that are used to approximate the frequency dependence of the forward and backward power spectral densities (22). Both sets should "adequately" cover the frequency range (25). The simplest choices are piecewise constant functions or hat functions associated with grid points for the frequency range (25). Furthermore, the grid points need not be spaced equi-distantly. In particular, it is possible to use some "spike-like" basis functions that mimic the spikes in the power spectral densities due to signals and pumps; cf. Figure 2. We stress that our approach allows two different sets of basis functions for the forward and backward waves. We remark that the number of basis functions (51) is roughly equal to a small multiple of the number of signal channels. Thus, even for state-of-the-art broadband Raman systems, the numbers l^+ and l^- typically will not exceed 1000.

Once the basis functions (51) are chosen, one employs the following ansatz for forward and backward power spectral densities:

$$\rho^+(z,t,\nu) = \sum_{j=0}^{l^+} y_j^+(z,t) f_j^+(\nu) \quad \text{and} \quad \rho^-(z,t,\nu) = \sum_{k=0}^{l^-} y_k^-(z,t) f_k^-(\nu). \tag{52}$$

The task then is to determine equations for the coefficient functions $y_j^+(z,t)$ and $y_k^-(z,t)$ in (52). In the following, we will use the vector notation

$$y^+(z,t) := \begin{bmatrix} y_0^+(z,t) \\ y_1^+(z,t) \\ \vdots \\ y_{l^+}^+(z,t) \end{bmatrix} \quad \text{and} \quad y^-(z,t) := \begin{bmatrix} y_0^-(z,t) \\ y_1^-(z,t) \\ \vdots \\ y_{l^-}^-(z,t) \end{bmatrix} \tag{53}$$

for these coefficient functions.

To obtain suitable equations for (53), we employ a standard Galerkin approach. First, we insert the ansatz (52) into (45)–(50). Then, the first equation, (45)–(47), is multiplied by each of the "forward" basis functions $f_i^+(\nu)$, $i = 0, 1, \ldots, l^+$, and subsequently integrated over the frequency range $\nu_{\min} \leq \nu \leq \nu_{\max}$. Similarly, the second equation, (48)–(50), is multiplied by each of the "backward" basis functions $f_i^-(\nu)$, $i = 0, 1, \ldots, l^-$, and subsequently integrated over $\nu_{\min} \leq \nu \leq \nu_{\max}$. The result is a set of $l^+ + l^- + 2$ coupled partial differential equations for the unknown $l^+ + l^- + 2$ entries of the vectors (53).

To formulate these equations, we introduce some more notation. For any integrable function $p(\nu)$, we set

$$A^+(p) := \left[\int_\nu f_i^+(\nu) f_j^+(\nu)\, p(\nu)\, d\nu \right]_{i,j=0,1,\ldots,l^+}, \tag{54}$$

$$A^-(p) := \left[\int_\nu f_i^-(\nu) f_j^-(\nu)\, p(\nu)\, d\nu \right]_{i,j=0,1,\ldots,l^-}, \tag{55}$$

$$A^\circ(p) := \left[\int_\nu f_i^+(\nu) f_j^-(\nu)\, p(\nu)\, d\nu \right]_{i=0,1,\ldots,l^+;\, j=0,1,\ldots,l^-}. \tag{56}$$

With $b_T(\nu,\zeta)$ denoting the function (43), we set

$$B^+ := 2h\left[\int_\nu\int_\zeta \nu f_i^+(\nu) f_j^+(\zeta)\, b_T(\nu,\zeta)\, d\zeta\, d\nu\right]_{i,j=0,1,\dots,l+}, \tag{57}$$

$$B^- := 2h\left[\int_\nu\int_\zeta \nu f_i^-(\nu) f_j^-(\zeta)\, b_T(\nu,\zeta)\, d\zeta\, d\nu\right]_{i,j=0,1,\dots,l^-}, \tag{58}$$

$$B_+^\circ := 2h\left[\int_\nu\int_\zeta \nu f_i^+(\nu) f_j^-(\zeta)\, b_T(\nu,\zeta)\, d\zeta\, d\nu\right]_{i=0,1,\dots,l+;\, j=0,1,\dots,l^-}, \tag{59}$$

$$B_-^\circ := 2h\left[\int_\nu\int_\zeta \nu f_i^-(\nu) f_j^+(\zeta)\, b_T(\nu,\zeta)\, d\zeta\, d\nu\right]_{i=0,1,\dots,l^-;\, j=0,1,\dots,l+}. \tag{60}$$

Let $a(\nu,\zeta)$ be the function defined in (42). For $k=0,1,\dots,l^+$, we set

$$C_k^+ := \left[\int_\nu\int_\zeta f_i^+(\nu) f_j^+(\nu)\, a(\nu,\zeta)\, f_k^+(\zeta) d\zeta\, d\nu\right]_{i,j=0,1,\dots,l+}, \tag{61}$$

$$D_k^- := \left[\int_\nu\int_\zeta f_i^-(\nu) f_j^-(\nu)\, a(\nu,\zeta)\, f_k^+(\zeta) d\zeta\, d\nu\right]_{i,j=0,1,\dots,l^-}, \tag{62}$$

and for $k=0,1,\dots,l^-$, we set

$$C_k^- := \left[\int_\nu\int_\zeta f_i^-(\nu) f_j^-(\nu)\, a(\nu,\zeta)\, f_k^-(\zeta) d\zeta\, d\nu\right]_{i,j=0,1,\dots,l^-}, \tag{63}$$

$$D_k^+ := \left[\int_\nu\int_\zeta f_i^+(\nu) f_j^+(\nu)\, a(\nu,\zeta)\, f_k^-(\zeta) d\zeta\, d\nu\right]_{i,j=0,1,\dots,l+}. \tag{64}$$

Note that the matrices

$$A^+(p), \quad C_0^+, C_1^+, \dots, C_{l+}^+, \quad D_0^+, D_1^+, \dots, D_{l-}^+ \tag{65}$$

all have the same sparsity structure. Similarly, the matrices

$$A^-(p), \quad C_0^-, C_1^-, \dots, C_{l-}^-, \quad D_0^-, D_1^-, \dots, D_{l+}^- \tag{66}$$

all have the same sparsity structure. For example, if the basis functions (51) are all piecewise constants, then the matrices (65) and (66) are all diagonal. If the basis functions (51) are all hat functions, then the matrices (65) and (66) are all tridiagonal. For more general choices of basis functions (51), the matrices (65) and (66) are always banded, provided that the basis functions are properly ordered.

On the other hand, the four matrices (57)–(60) are dense in general. However, note that the order of all the matrices (54)–(64) is bounded by either $l^+ + 1$ or $l^- + 1$, which never exceeds 1000, and so these matrices are all small for today's standards.

Using the notation (54)–(64), the partial differential equations resulting from the Galerkin approach applied to (45)–(50) are as follows:

$$A^+(1)\,\frac{\partial y^+(z,t)}{\partial z} + A^+(1/v_{\mathrm{g}})\,\frac{\partial y^+(z,t)}{\partial t} = -A^+(\delta_T)\,y^+(z,t) + A^\circ(\gamma)\,y^-(z,t) \tag{67}$$

$$+\,B^+\,y^+(z,t) + B^\circ_+\,y^-(z,t) \tag{68}$$

$$+\sum_{k=0}^{l^+}\big(C_k^+\,y^+(z,t)\big)y_k^+(z,t) + \sum_{k=0}^{l^-}\big(D_k^+\,y^+(z,t)\big)y_k^-(z,t), \tag{69}$$

$$A^-(1)\,\frac{\partial y^-(z,t)}{\partial z} - A^-(1/v_{\mathrm{g}})\,\frac{\partial y^-(z,t)}{\partial t} = A^-(\delta_T)\,y^-(z,t) - \big(A^\circ(\gamma)\big)^T y^+(z,t) \tag{70}$$

$$-\,B^-\,y^-(z,t) - B^\circ_-\,y^+(z,t) \tag{71}$$

$$-\sum_{k=0}^{l^-}\big(C_k^-\,y^-(z,t)\big)y_k^-(z,t) - \sum_{k=0}^{l^+}\big(D_k^-\,y^-(z,t)\big)y_k^+(z,t). \tag{72}$$

These equations are completed by the Galerkin projections of the initial conditions (40) and (41). More precisely, the functions $r_0(t,\nu)$ and $r_1(t,\nu)$ from (40) and (41) are used to define the right-hand sides of the following time-dependent linear systems:

$$A^+(1)\,y_0(t) = \left[\int_\nu f_i^+(\nu) r_0(t,\nu)\,d\nu\right]_{i=0,1,\ldots,l^+}, \tag{73}$$

$$A^-(1)\,y_1(t) = \left[\int_\nu f_i^-(\nu) r_1(t,\nu)\,d\nu\right]_{i=0,1,\ldots,l^-}. \tag{74}$$

Let $y_0(t)$ and $y_1(t)$ denote the solutions of the linear systems (73) and (74), respectively. The initial conditions for the partial differential equations (67)–(71) are then as follows:

$$y^+(0,t) = y_0(t) \quad \text{and} \quad y^-(L,t) = y_1(t). \tag{75}$$

Note that the system (67)–(72) and (75) is just a time-dependent two-point boundary-value problem. Indeed, let us define

$$M := \begin{bmatrix} A^+(1) & 0 \\ 0 & A^-(1) \end{bmatrix}, \quad N := \begin{bmatrix} A^+(1/v_{\mathrm{g}}) & 0 \\ 0 & -A^-(1/v_{\mathrm{g}}) \end{bmatrix}, \tag{76}$$

$$F^+(y^+,y^-) := -\big(A^+(\delta_T) - B^+\big)y^+ + \big(A^\circ(\gamma) + B^\circ_+\big)y^- + \sum_{k=0}^{l^+}\big(C_k^+\,y^+\big)y_k^+ + \sum_{k=0}^{l^-}\big(D_k^+\,y^+\big)y_k^-, \tag{77}$$

$$F^-(y^+,y^-) := \big(A^-(\delta_T) - B^-\big)y^- - \Big(\big(A^\circ(\gamma)\big)^T + B^\circ_-\Big)y^+ - \sum_{k=0}^{l^-}\big(C_k^-\,y^-\big)y_k^- - \sum_{k=0}^{l^+}\big(D_k^-\,y^-\big)y_k^+. \tag{78}$$

With this notation, the system (67)–(72) and (75) can be stated as follows:

$$M \frac{\partial}{\partial z} \begin{bmatrix} y^+(z,t) \\ y^-(z,t) \end{bmatrix} + N \frac{\partial}{\partial t} \begin{bmatrix} y^+(z,t) \\ y^-(z,t) \end{bmatrix} = \begin{bmatrix} F^+\left(y^+(z,t), y^-(z,t)\right) \\ F^-\left(y^+(z,t), y^-(z,t)\right) \end{bmatrix}, \tag{79}$$

$$y^+(0,t) = y_0(t) \quad \text{and} \quad y^-(L,t) = y_1(t). \tag{80}$$

We remark that the steady-state case is obtained by choosing constant (in time) initial conditions y_0 and y_1. In this case, the solution of (79) and (80) is independent of time, and we set $y^+(z) := y^+(z,t)$ and $y^-(z) := y^-(z,t)$. The equations (79) and (80) then simplify to the following form:

$$M \frac{\partial}{\partial z} \begin{bmatrix} y^+(z) \\ y^-(z) \end{bmatrix} = \begin{bmatrix} F^+\left(y^+(z), y^-(z)\right) \\ F^-\left(y^+(z), y^-(z)\right) \end{bmatrix}, \tag{81}$$

$$y^+(0) = y_0 \quad \text{and} \quad y^-(L) = y_1. \tag{82}$$

Problem (81) and (82) is a standard two-point boundary value problem. Such problems and numerical techniques for their solution have been studied extensively; see, e.g., [13, 15], [30, Chapter 7] and the references given there. Numerical techniques include the multiple shooting method, collocation methods, and Galerkin methods (in z).

In the general, time-dependent case, problem (79) and (80) simplifies somewhat if one neglects the frequency dependence of the group velocity $v_{\mathrm{g}}(\nu)$. Indeed, if v_{g} is treated as a constant, then

$$A^+(1/v_{\mathrm{g}}) = \frac{1}{v_{\mathrm{g}}} A^+(1) \quad \text{and} \quad A^-(1/v_{\mathrm{g}}) = \frac{1}{v_{\mathrm{g}}} A^-(1).$$

In this case, the differential equations (79) and (80) can be written as follows:

$$\frac{\partial}{\partial z} \begin{bmatrix} y^+(z,t) \\ y^-(z,t) \end{bmatrix} + \frac{1}{v_{\mathrm{g}}} \frac{\partial}{\partial t} \begin{bmatrix} y^+(z,t) \\ -y^-(z,t) \end{bmatrix} = M^{-1} \begin{bmatrix} F^+\left(y^+(z,t), y^-(z,t)\right) \\ F^-\left(y^+(z,t), y^-(z,t)\right) \end{bmatrix}, \tag{83}$$

$$y^+(0,t) = y_0(t) \quad \text{and} \quad y^-(L,t) = y_1(t). \tag{84}$$

Solutions of the system (83) and (84) can be computed efficiently by means of the method of characteristics; see, e.g., [7, Chapters 8 and 9], [10, Chapter 9], and [26, Chapter 14].

5 Concluding remarks

We have presented a general formulation of the system of differential equations that describe the power evolution in Raman fiber amplifiers. The unknowns in these equations are the power spectral densities of the forward and backward propagating waves as functions of position along the fiber, time, and frequency. We have also outlined a Galerkin approach for discretizing the equations in frequency space. This results in a standard system of hyperbolic partial differential equations in only position along the fiber and time. The choice of the basis functions used in the Galerkin approach and details of an efficient implementation of a method of characteristics for solving the resulting hyperbolic systems will be described elsewhere.

A Raman simulator based on the equations and the Galerkin approach presented in this paper is currently being developed by Todd Salamon and others.

Acknowledgments

I would like to thank Lawrence Cowsar, Daniel Fishman, Tin Kam Ho, Todd Salamon, Leon Vardapetyan, and Christopher White for numerous discussions on various aspects of simulation of Raman amplification. I am grateful to Narasimhan Raghavan for performing measurements on an actual DWDM system and providing the data shown in Figure 2.

References

[1] G. P. Agrawal. *Fiber-Optic Communication Systems.* Wiley Series in Microwave and Optical Engineering. John Wiley & Sons, Inc., New York, second edition, 1997.

[2] C.-J. Chen and W. S. Wong. Transient effects in saturated Raman amplifiers. *Electron. Lett.*, 37(6):371–373, 2001.

[3] C.-J. Chen, J. Ye, W. S. Wong, Y.-W. Lu, M.-C. Ho, Y. Cao, M. J. Gassner, J. S. Pease, H.-S. Tsai, H. K. Lee, S. Cabot, and Y. Sun. Control of transient effects in distributed and lumped Raman amplifiers. *Electron. Lett.*, 37(21):1304–1305, 2001.

[4] Y. Emori, S. Kado, and S. Namiki. Broadband flat-gain and low-noise Raman amplifiers pumped by wavelength-multiplexed high-power laser diodes. *Opt. Fiber Technol.*, 8:107–122, 2002.

[5] Y. Emori and S. Namiki. Broadband Raman amplifier for WDM. *IEICE Trans. Commun.*, E84-B(5):1219–1223, 2001.

[6] G. Goeger and B. Lankl. Techniques for suppression of Raman and EDFA gain transients in dynamically switched transparent photonic networks. In *Technical Digest of the 28th European Conference on Optical Communication*, volume 3, 2002.

[7] B. Gustafsson, H.-O. Kreiss, and J. Oliger. *Time dependent problems and difference methods.* John Wiley & Sons, Inc., New York, 1995.

[8] A. Hasegawa. Numerical study of optical soliton transmission amplified periodically by the stimulated Raman process. *Appl. Opt.*, 23(19):3302–3309, 1984.

[9] T. K. Ho, L. C. Cowsar, R. W. Freund, L. Vardapetyan, and T. R. Salamon. Modeling and simulation of control dynamics in optical transport systems. Technical Memorandum No. 10009640-020925-32TM, Bell Laboratories, Lucent Technologies, Murray Hill, New Jersey, USA, September 2002.

[10] C. Johnson. *Numerical solution of partial differential equations by the finite element method.* Cambridge University Press, New York, 1987.

[11] M. Karásek. Fast power transients in Raman fibre amplifiers. In *Proceedings of the 4th International Conference on Transparent Optical Networks*, pages 122–127. IEEE, 2002.

[12] S. V. Kartalopoulos. *Introduction to DWDM Technology: Data in a Rainbow.* IEEE Press, New York, 2000.

[13] H. B. Keller. *Numerical methods for two-point boundary-value problems.* Dover Publications, New York, 1992.

[14] H. Kidorf, K. Rottwitt, M. Nissov, M. Ma, and E. Rabarijaona. Pump interactions in a 100-nm bandwidth Raman amplifier. *IEEE Photon. Technol. Lett.*, 11(5):530–532, 1999.

[15] J. Kierzenka and L. F. Shampine. A BVP solver based on residual control and the Matlab PSE. *ACM Trans. Math. Software*, 27(3):299–316, 2001.

[16] A. J. Lowery. Photonic simulation tools. In I. P. Kaminow and T. Li, editors, *Optical Fiber Telecommunications, Volume IV B Systems and Impairments*, pages 564–610. Academic Press, San Diego, 2002.

[17] M. Menif, M. Karásek, and L. A. Rusch. Cross-gain modulation in Raman fiber amplifier: experimentation and modeling. *IEEE Photon. Technol. Lett.*, 14(9):1261–1263, 2002.

[18] D. L. Mills. *Nonlinear Optics.* Springer-Verlag, Berlin, Germany, second edition, 1998.

[19] B. Min, W. J. Lee, and N. Park. Efficient formulation of Raman amplifier propagation equations with average power analysis. *IEEE Photon. Technol. Lett.*, 12(11):1486–1488, 2000.

[20] L. Mollenauer, J. Gordon, and M. Islam. Soliton propagation in long fibers with periodically compensated loss. *IEEE J. Quantum Electron.*, QE-22(1):157–173, 1986.

[21] L. Mollenauer and K. Smith. Demonstration of soliton transmission over more than 4000 km in fiber with loss periodically compensated by Raman gain. *Opt. Lett.*, 13(8):675–677, 1988.

[22] S. Namiki and Y. Emori. Ultrabroad-band Raman amplifiers pumped and gain-equalized by wavelength-division-multiplexed high-power laser diodes. *IEEE J. Select. Topics Quantum Electron.*, 7(1):3–16, 2001.

[23] A. Penzkofer, A. Laubereau, and W. Kaiser. High intensity Raman interactions. *Prog. Quant. Electr.*, 6:55–140, 1979.

[24] V. E. Perlin and H. G. Winful. On distributed Raman amplification for ultrabroad-band long-haul WDM systems. *J. Lightwave Technol.*, 20(3):409–416, 2002.

[25] V. E. Perlin and H. G. Winful. Optimal design of flat-gain wide-band fiber Raman amplifiers. *J. Lightwave Technol.*, 20(2):250–254, 2002.

[26] A. Quarteroni and A. Valli. *Numerical approximation of partial differential equations.* Springer-Verlag, Berlin, 1994.

[27] R. Ramaswami and K. N. Sivarajan. *Optical Networks: A Practical Perspective.* Morgan Kaufmann, San Francisco, second edition, 2002.

[28] K. Rottwitt and A. J. Stentz. Raman amplification in lightwave communication systems. In I. P. Kaminow and T. Li, editors, *Optical Fiber Telecommunications, Volume IV A Components*, pages 213–257. Academic Press, San Diego, 2002.

[29] Y. R. Shen. *The principles of nonlinear optics.* John Wiley & Sons, Inc., New York, 1984.

[30] J. Stoer and R. Bulirsch. *Introduction to Numerical Analysis.* Springer-Verlag, New York, second edition, 1993.

[31] R. H. Stolen. Polarization effects in fiber Raman and Brillouin lasers. *IEEE J. Quantum Electron.*, 15(10):1157–1160, 1979.

[32] R. H. Stolen. Nonlinearity in fiber transmission. *Proc. IEEE*, 68(10):1232–1236, 1980.

[33] R. H. Stolen, C. Lee, and R. K. Jain. Development of the stimulated Raman spectrum in single-mode silica fibers. *J. Opt. Soc. Amer. B*, 1(4):652–657, 1984.

[34] Y. Sugaya, S. Muro, Y. Sato, and E. Ishikawa. Suppression method of transient power response of raman amplifier caused by channel add-drop. In *Technical Digest of the 28th European Conference on Optical Communication*, volume 2, 2002.

[35] W. P. Urquhart and P. J. Laybourn. Effective core area for stimulated Raman scattering in single-mode optical fibres. *IEE Proceedings-J Optoelectronics*, 132(4):201–204, 1985.

[36] L. Vardapetyan. Equations in FROG: a simplified approach to modeling propagation in Raman and erbium-doped fiber. Unpublished notes, 2002.

[37] M. Yan, J. Chen, W. Jiang, J. Li, J. Chen, and X. Li. Automatic design scheme for optical-fiber Raman amplifiers backward-pumped with multiple laser diode pumps. *IEEE Photon. Technol. Lett.*, 13(9):948–950, 2001.

[38] X. Zhou, C. Lu, P. Shum, and T. Cheng. A simplified model and optimal design of a multiwavelength backward-pumped fiber Raman amplifier. *IEEE Photon. Technol. Lett.*, 13(9):945–947, 2001.